Biochimica et Biophysica Acta, 1056 (1991) 259–272

ADONIS 000527289100071Z

BBABIO 43328

Heterogeneity of kinetics and electron transfer equilibria in the bacteriopheophytin and quinone electron acceptors of reaction centers from *Rhodopseudomonas viridis*

Ji-Liang Gao, Robert J. Shopes * and Colin A. Wraight

Department of Physiology and Biophysics and Department of Plant Biology, University of Illinois, Urbana, IL (U.S.A.)

(Received 13 June 1990)
(Revised manuscript received 9 October 1990)

Key words: Reaction center; Charge recombination; Conformation; Bacteriopheophytin; Quinone; (*Rps. viridis*)

The decay of the charge separated state, $P^+Q_AQ_B^-$, produced in a flash, was measured in reaction centers from *Rhodopseudomonas viridis* supplemented with ubiquinone to reconstitute secondary quinone (Q_B) activity. The decay occurs by recombination via the state $P^+Q_A^-Q_B$ which has an inherent recombination rate constant (k_{QA}) of about 10^3 s^{-1}. The observed rate of decay of $P^+Q_AQ_B^-$ is therefore controlled by the electron transfer equilibrium (K_2) between $P^+Q_AQ_B^-$ and $P^+Q_A^-Q_B$: $k_{QB} = k_{QA}[1 + K_2]^{-1}$. The decay of $P^+Q_AQ_B^-$ was biphasic in the same manner as previously found for the much faster recombination of $P^+Q_A^-$ in reaction centers lacking functional Q_B (Sebban, P. and Wraight, C.A. (1989) Biochim. Biophys. Acta 974, 54–65). The decay kinetics of both processes were well fit by sums of two exponential components with rate constants that differed by a factor of about 5. Comparison of the fast phase of $P^+Q_AQ_B^-$ decay (k_{QB}^{fast}) with the fast phase of $P^+Q_A^-$ decay (k_{QA}^{fast}), or of k_{QB}^{slow} with k_{QA}^{slow}, yielded very similar values for K_2 over a wide range of pH, temperature and salt concentration. Thus, the source of the heterogeneity in the recombination kinetics does not significantly perturb the energetics of the Q_A to Q_B electron transfer equilibrium. As a function of pH, K_2 decreased from a value of about 10^3 at pH 5 to a minimum of 10^2 at pH 8. It then increased to about 250 at pH 10, before decreasing again at higher pH. This complex behavior was satisfactorily described by the influence of four independent ionizable groups with differential effects on the stability of the $P^+Q_A^-Q_B$ and $P^+Q_AQ_B^-$ states, i.e., $pK_{QA^-} \neq pK_{QB^-}$. The temperature dependence of K_2, at pH 8.5, revealed $\Delta H^\circ = -0.35$ eV and $\Delta S^\circ = -0.75$ meV/deg ($-T\Delta S^\circ = 0.22$ eV at 296 K). This large entropy change is most likely related to proton binding events accompanying the electron transfer. The salt dependence of K_2 was substantial due to opposing effects on the recombination rates: k_{QB} decreased with increasing salt concentration, while k_{QA} increased. This is interpreted as reflecting the influence of surface pH and solvent dielectric on the species I/I^-, Q_A/Q_A^- and Q_B/Q_B^-. The relative amplitudes of the fast and slow components of the $P^+Q_AQ_B^-$ recombination were also dependent on pH, temperature and salt concentration and followed closely the heterogeneity of the $P^+Q_A^-$ recombination. The source of the components is ascribed to a slow, proton-linked equilibrium between two conformational states of the protein (conformers), $C_f \leftrightarrow C_s$, that differ in their $P^+Q_A^-$ recombination rates (k_{QA}^{fast} and k_{QA}^{slow}). The equilibrium between the states is established before the flash and readjusts, after the flash, in a few seconds – a time scale longer than the $P^+Q_AQ_B^-$ lifetime ($\leqslant 1$ s). The conformational equilibrium constant, K_{cs}, varied with pH in a complex way that roughly correlated with the pH dependence of K_2, suggesting that the quinone electron transfer equilibrium and the interconversion of the two conformers (fast and slow) may be sensitive to some of the same protonation events. The temperature dependence of K_{cs} was slight but corresponded to $\Delta H^\circ = -60$ meV and $\Delta S^\circ = -0.17$ meV/deg ($-T\Delta S^\circ = 50$ meV at 296 K). It is suggested that the fast and slow conformers may differ in the energy gap between $P^+Q_A^-$ and P^+I^-, but differences in the intrinsic decay rate of P^+I^- may also contribute. If the source of the heterogeneity is energetic, the major contribution to the variation is likely to be the energy level of P^+I^-. Variability in the kinetic behavior was observed in different reaction center preparations, some exhibiting rates of $P^+Q_A^-$ recombination (both phases) and Cyt $c^+Q_A^-$ decay that are 2–2.5-fold faster, without any corresponding acceleration of the

* Present address: Stratacyte Inc., La Jolla, CA, U.S.A.

Correspondence: C.A. Wraight, Department of Plant Biology, University of Illinois, 505 S. Goodwin Ave, Urbana, IL 61801, U.S.A.

$P^+Q_AQ_B^-$ decay rates. The origin of this effect is unknown but it is suggested that it reflects an increase in the free energy level of the $P^+Q_A^-$ state by 20–25 meV, simultaneously decreasing the gap between $P^+Q_A^-$ and P^+I^- and increasing that between $P^+Q_A^-Q_B$ and $P^+Q_AQ_B^-$.

Introduction

The primary events of photosynthesis in reaction centers from purple bacteria are now becoming well characterized, and the structure of the reaction center (RC) from two species, *Rhodopseudomonas viridis* and *Rhodobacter sphaeroides,* is known at atomic resolution [1–4]. The core of the RC consists of two partially homologous subunits, L and M, which bind all the cofactors involved in the photochemical charge separation. A third subunit, H, caps this structure and may be important in stabilizing the whole complex and in facilitating proton uptake that accompanies later stages of the charge stabilization events. The photochemical, primary electron donor consists of a dimer of bacteriochlorophylls ($BChl_2$ or P). Within a few picoseconds following excitation to the first excited singlet state, P* transfers an electron to the bacteriopheophytin (BPh or I) bound to the L-subunit. Subsequently, the electron is transferred to the primary quinone, Q_A, forming $P^+Q_A^-$. Reaction centers from *Rps. viridis* have a fourth subunit containing four *c*-type hemes, capable of rapid electron transfer to P^+. If these hemes are chemically oxidized before the flash, the state $P^+Q_A^-$ is relativley long-lived and decays by recombination in about 1 ms [5,6].

We have previously shown that in *Rps. viridis* the state $P^+Q_A^-$ recombines via two parallel routes, at room temperature: a direct and activationless recombination between P^+ and Q_A^-, and a thermally activated process via the state P^+I^- [6]. This is in contrast to native RCs from *Rb. sphaeroides,* where the recombination occurs almost exclusively via the direct, activationless route [7,8]. The distinction arises most probably from the lower excitation levels of BChl *b* and BPh *b* in *Rps. viridis* compared to BChl *a* and BPh *a* in *Rb. sphaeroides,* although the presence of menaquinone as Q_A in *Rps. viridis* and ubiquinone in *Rb. sphaeroides* may also contribute. The result of these substitutions is to decrease the free energy gap between $P^+Q_A^-$ and P^+I^- so that the latter is thermally accessible at room temperature. Very rapid decay to the ground state ($k_d = (2\text{–}8)\cdot 10^7\ s^{-1}$) then ensures a significant contribution from this path. The observed decay, k_{QA}, is given by the sum of these two contributing paths, according to Ref. 6:

$$k_{QA} = k_d \cdot \exp(-\Delta G^\dagger / k_b T) + k_T \qquad (1)$$

where $\Delta G^\dagger$ is the free energy gap between $P^+Q_A^-$ and P^+I^-, k_b is Boltzmann's constant and k_T is the rate constant for the activationless, direct recombination process observed alone at low temperature.

More recently we reported that the decay of $P^+Q_A^-$ is generally not a single exponential component but is at least biphasic, reflecting heterogeneity in the RC population [9]. Similar behavior was reported by Parot et al. [10]. The kinetics were analysed as biexponential and the amplitudes of the fast and slow components shown to exhibit slightly different spectra and to vary with pH and temperature, indicating interconversion between two distinct subpopulations. The dependence of the rates on pH was interpreted in terms of different protonation states of the protein, with distinct energetic influences on the redox potentials of I/I^- and Q_A/Q_A^-, resulting in different activation energies for the activated recombination path. Also, since the recombination in *Rps. viridis* is so fast ($k_{QA} \approx 10^3\ s^{-1}$), it was suggested that at alkaline pH ($\geqslant 7$) the protonation equilibria were not fully established during the lifetime of $P^+Q_A^-$, thereby contributing to the observed non-exponential (heterogeneous) decay kinetics [9].

If lack of protonation equilibrium on the milliseconds timescale were truly the source of heterogeneity of the $P^+Q_A^-$ decay, it might be expected that a much slower decay process would not manifest complex kintics, as protonation equilibria are generally quite fast. Proper equilibration would lead to monoexponential kinetics reflecting a time average over the various protonation states present. The decay of the $P^+Q_AQ_B^-$ state (abbreviated as $P^+Q_B^-$) is known to proceed via $P^+Q_A^-$ in *Rb. sphaeroides* [11,12] and *Rps. viridis* [13]. The rate of decay of $P^+Q_B^-$ is about 1–10 s^{-1} in *Rps. viridis,* making it a good candidate to test the rapidity of the protonation equilibria involved in the $P^+Q_A^-$ kinetics. The results are reported here and the conclusion – that the heterogeneity of the $P^+Q_A^-$ decay is still observed in the $P^+Q_B^-$ recombination – has significant implications for the analysis of RC behavior.

Methods

Reaction centers were isolated and purified from *Rps. viridis* as described previously [5]. The kinetics of $P^+Q_A^-$ and $P^+Q_B^-$ recombination following a flash were measured as the decay of the P^+ absorbance signal at 450 nm, using a kinetic spectrophotometer of local design. The bound cytochromes were chemically oxidized by the addition of 5 mM potassium ferricyanide to the RC stock, followed by extensive dialysis overnight to remove the ferricyanide. Samples in the measuring cuvette contained 1–2 μM RCs and less than

0.1 μM ferricyanide. The low ferricyanide concentration was necessary to avoid rapid oxidation of Q_A^-, which occurs at pH values below 9 [14]. 10 μM ubiquinone (Q-10) was added to the sample to reconstitute secondary acceptor quinone activity which is largely lost during the RC purification procedure [5]. The native ubiquinone is Q-9, but Q-10 is functionally equivalent [5]. For measurements of pH dependences, the sample pH was adjusted with small additions of HCl and NaOH, and the assay medium contained 1 mM phosphate buffer.

Exponential analyses of the kinetics were performed using a modified Marquardt algorithm run on an LSI 11/73 computer (DEC) that was also used for the data acquisition, as described elsewhere [15].

Results

Analysis of the kinetics of charge recombination

Fig. 1 shows the kinetics of recombination of the $P^+Q_B^-$ state, measured as the decay of P^+ in RCs supplemented with ubiquinone (Q-10), at pH 8.5 and 23° C. The decay curve was well fit by the sum of two exponentials with decay rates of 11.3 s^{-1} (k_{QB}^{fast}) and 2.75 s^{-1} (k_{QB}^{slow}), and relative amplitudes of 0.35 and 0.65, respectively. A small constant term was also fitted; it was usually less than 5% of the initial amplitude. We consider it most likely to arise from a small amount of oxidation of Q_B^- by exogenous oxidants (including oxygen), leaving a long-lived P^+ signal [14]. The rates of the two exponential components differed by a factor of 4–6 over a wide range of conditions. A very similar biphasicity was seen for the kinetics of charge recombination in the $P^+Q_A^-$ state, with 4 mM *o*-phenanthroline [9] and this is shown in Fig. 1 for comparison. The $P^+Q_A^-$ decay was fit by the sum of two exponentials with decay rates of 1255 s^{-1} (k_{QA}^{fast}) and 330 s^{-1} (k_{QA}^{slow}), and relative amplitudes of 0.35 and 0.65. The constant term was always less than 5% and most likely of the same origin as for $P^+Q_B^-$ – the rate of oxidation of Q_A^- by exogenous oxidants is much faster than that of Q_B^- [14], so the relative contribution is similar in spite of the much faster recombination rate of $P^+Q_A^-$.

Some quantitative variability was observed in the kinetics of different RC preparations from *Rps. viridis*, some having $P^+Q_A^-$ recombination rates (both fast and slow phases) 2–2.5-fold higher than others. The $P^+Q_B^-$ recombination rates, on the other hand, did not differ, so the values of K_2 calculated for the two types of preparation also varied by a factor of about 2. The pH and temperature dependences of K_2, however, were almost indistinguishable in the two types of RC preparation and data from both types are used in this work. Significantly, preparations which displayed faster $P^+Q_A^-$ recombination rates showed faster recovery from the cyt $c^+Q_A^-$ state, generated in samples with only the high potential cytochromes reduced before the flash. This reaction also proceeds via recombination of $P^+Q_A^-$ [16]. The source of the variability in these preparations is still obscure.

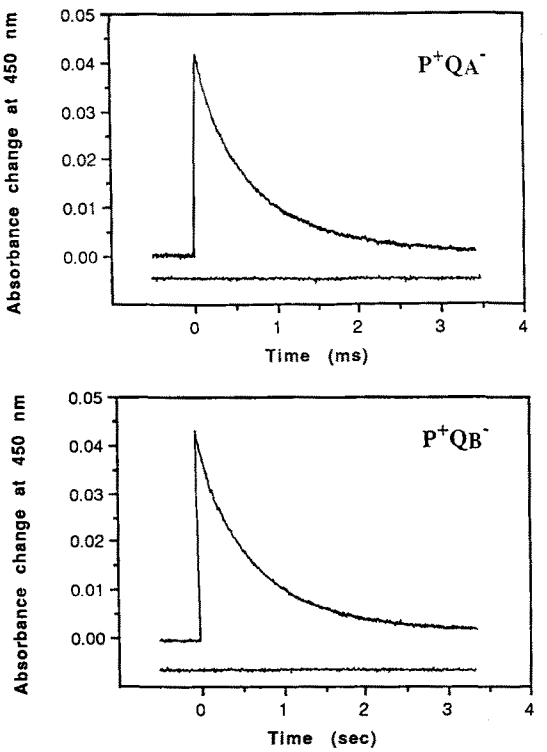

Fig. 1. Kinetics of charge recombination in isolated reaction centers from *Rps. viridis*, measured at 450 nm. Top: $P^+Q_A^-$ charge recombination; the kinetics were fit with two exponential components with decay rates of 1255 s^{-1} (k_{QA}^{fast}) and 330 s^{-1} (k_{QA}^{slow}), and relative amplitudes of 0.35 and 0.65, respectively, plus a constant (3.8% of the initial amplitude). Bottom: $P^+Q_B^-$ charge recombination; the kinetics were fit with two exponential components, with decay rates of 11.3 s^{-1} (k_{QB}^{fast}) and 2.75 s^{-1} (k_{QB}^{slow}), and relative amplitudes of 0.35 and 0.65, respectively, plus a constant (5.5% of the initial amplitude). The residuals from the biexponential fits are shown below each trace. Conditions: approx. 1 μM RCs in 1 mM phosphate buffer (pH 8.5), 100 mM NaCl, 0.05% Triton X-100, 23°C; $P^+Q_A^-$, plus 4 mM *o*-phenanthroline; $P^+Q_B^-$, plus 10 μM ubiquinone-10 (Q-10).

The complexity of the kinetics is inherent to the recombination process rather than arising from interference from electron donation or acceptance by exogenous components. Even when ferricyanide was present (approx. 30 μM at high pH), the expected rate of Q_B^- oxidation was much slower than the measured P^+ decay [14]. Similarly, the rate of donation from the low levels of ferrocyanide present (approx. 3 μM at $E_h \approx 460$ mV) was also much slower than the time range of $P^+Q_B^-$ recombination [14]. It might be considered that the decay could be non-exponential or polyphasic rather than biphasic, but attempts to fit the data with three exponentials did not consistently improve the residuals, and the amplitude of the third component varied apparently randomly in the range of 1–5% of the total.

Temperature dependence of the decay kinetics

The temperature dependence of the $P^+Q_B^-$ recombination kinetics was measured in aqueous buffer, at pH 8.5, between 273 and 300 K (Fig. 2). The decay rates of the two components decreased with decreasing temperature, from 3.5 s^{-1} and 12.5 s^{-1} at 300 K to 0.5 s^{-1} and 1.6 s^{-1} at 273 K. Arrhenius plots of the data showed good linearity, with slopes equivalent to apparent activation energies of 0.506 ± 0.012 eV and 0.557 ± 0.012 eV for the slow and fast components, respectively. The $P^+Q_A^-$ recombination was also measured under equivalent conditions and the slopes of the Arrhenius plots were equivalent to apparent activation energies of 0.155 ± 0.008 eV and 0.199 ± 0.004 eV for the slow and fast components, respectively. The amplitudes of the $P^+Q_B^-$ kinetic phases were only slightly temperature-dependent, the fast component increasing from 30% at 273 K to 40% at 300 K. This is shown in Fig. 2 (top), presented as an equilibrium constant (K_{cs}) for the interconversion between two conformational states (fast ↔ slow), as described in the Discussion.

pH dependence of the $P^+Q_B^-$ and $P^+Q_A^-$ decay kinetics

The rates of the two components of the P^+Q_B decay exhibited similar pH dependences and are shown in Fig. 3 (lower panel). At pH 6.0, the rates were 0.85 s^{-1} and

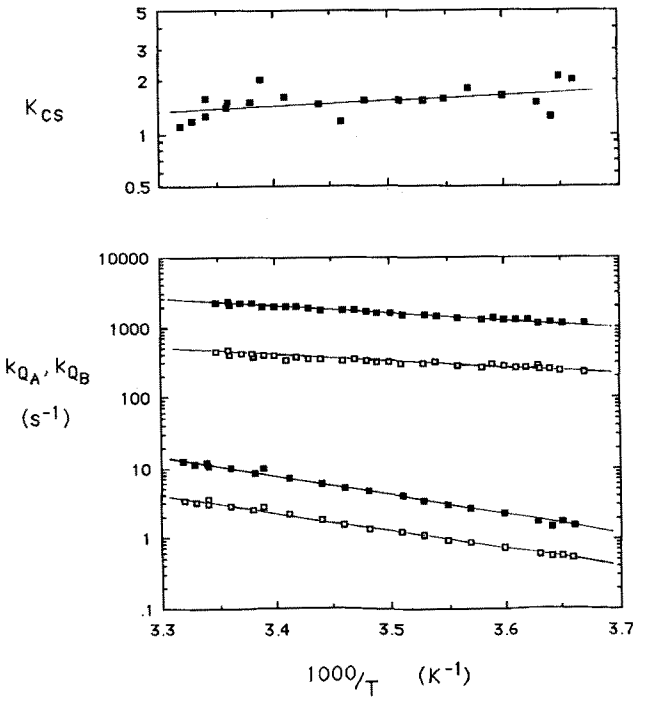

Fig. 2. Temperature dependence of the P^+ decay kinetics in the presence and absence of functional secondary quinone. Bottom panel: Rates of decay of $P^+Q_A^-$ (k_{QA}, upper data) and $P^+Q_B^-$ (k_{QB}, lower data) analysed as biexponential. Top panel: Relative amplitudes of the fast and slow components of the $P^+Q_B^-$ recombination kinetics presented as an equilibrium constant (K_{cs}) between two states, $C_f \leftrightarrow C_s$, as described in the text. ■, fast phase; □, slow phase. Conditions: as for Fig. 1 except 10 mM Tris (pH 8.5), instead of phosphate.

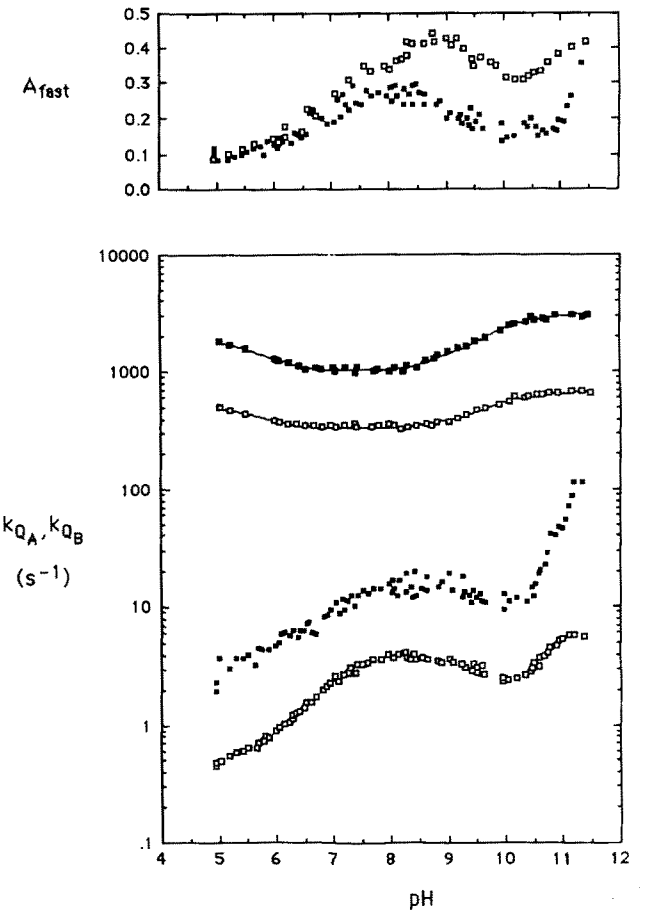

Fig. 3. pH dependence of the P^+ decay kinetics in the presence and absence of functional secondary quinone. Bottom panel: Rates of decay of $P^+Q_A^-$ (k_{QA}, upper data) and $P^+Q_B^-$ (k_{QB}, lower data) analysed as biexponential (■, fast phase; □, slow phase). Top panel: Amplitude of the fast phase of the $P^+Q_A^-$ (□) and $P^+Q_B^-$ (■) recombination kinetics (the slow phase amplitude, A_{slow}, is the complement of A_{fast}). Conditions: as for Fig. 1. Curves drawn through k_{QA} data according to Eqn. 5B, using the parameters given in Table II.

5.5 s^{-1}, and both increased with increasing pH to maximum values of 3.9 s^{-1} and 14 s^{-1} at pH 8.5. Above pH 8.5 both components slowed slightly to 2.5 s^{-1} and 10^{-1} at pH 10.3, and then increased again at even higher pH. The rates of the two components of the $P^+Q_A^-$ recombination process, obtained with *o*-phenanthroline present and in the absence of added Q-10, are also shown in Fig. 3.

The relative amplitudes of the two components of the $P^+Q_B^-$ decay also changed with pH. As shown in Fig. 3 (top), in 100 mM NaCl the contribution of the fast component was about 0.1 at pH 6.0 and increased to a maximum value of about 0.3 at pH 8–8.5. At higher pH it diminished in amplitude, to a local minimum at pH 10–10.5, and then increased again above pH 11. The relative amplitudes of the components of the $P^+Q_A^-$ decay exhibited similar but not identical behavior. At low pH (< 8) the $P^+Q_B^-$ and $P^+Q_A^-$ amplitudes were

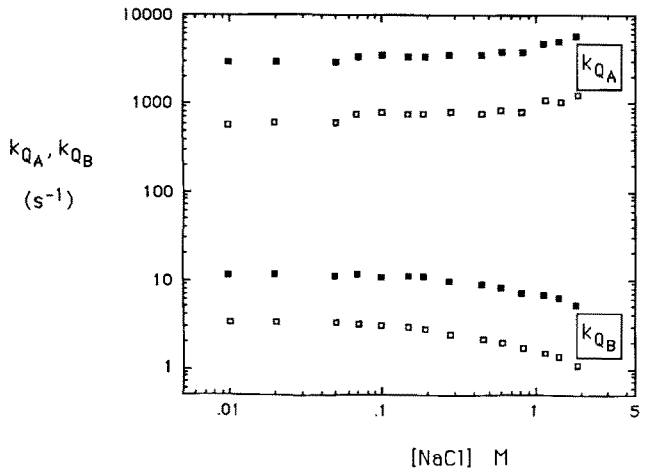

Fig. 4. Salt dependence of the P^+ decay kinetics in the presence and absence of functional secondary quinone. Rates of decay of $P^+Q_A^-$ (k_{QA}, upper data) and $P^+Q_B^-$ (k_{QB}, lower data) analysed as biexponential (■, fast phase; □, slow phase). Conditions: as for Fig. 2, except variable NaCl. The RC preparation used here was of the 'fast' variety.

almost superimposable, but at higher pH the relative amplitude of the fast phase was distinctly larger in the $P^+Q_A^-$ decay, although the general shape of the pH dependence was very similar.

Salt dependence of the decay kinetics

The two components of the $P^+Q_B^-$ recombination were significantly dependent on the salt concentration (Fig. 4). At pH 8.5, both rates decreased by 2–3 fold as the salt concentration was raised from 0.1 M to 2 M NaCl. By contrast, the rates of the two components of the $P^+Q_A^-$ recombination increased as the salt concentration was raised over the same range. The relative amplitudes of the two components of the $P^+Q_B^-$ recombination were quite markedly salt dependent and are presented below (Fig. 7) as the equilibrium constant, K_{cs}. At 2 M NaCl the kinetics of the $P^+Q_B^-$ decay were 90% slow.

Discussion

The kinetics of P^+ decay in the presence of added ubiquinone clearly manifests two phases over a wide range of conditions. The existence of a similar biphasicity over the very different timescales of the $P^+Q_A^-$ and $P^+Q_B^-$ recombination supports the notion of long-lived, kinetically distinct, but interconvertible, states of the RC, as more fully justified below, During the preparation of this manuscript a qualitatively similar study was reported by Sebban and co-workers, focusing on the pH dependence of the kinetics. They observed biphasic kinetics of $P^+Q_B^-$ recombination in chromatophores and proteoliposomes as well as in isolated reaction centers [17].

The $Q_A^-Q_B/Q_AQ_B^-$ equilibrium

In *Rb. sphaeroides,* the decay of the $P^+Q_B^-$ state is understandable as arising from a rapid electron transfer equilibrium with $P^+Q_A^-$, followed by recombination of that state [11,12,18,19]:

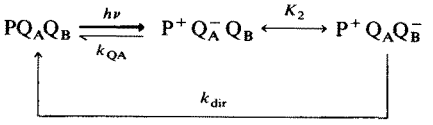

Scheme I.

Provided the direct electron transfer from Q_B^- to P^+ is negligible, the observed rate of recombination with functional Q_B is given by:

$$k_{QB} = k_{QA}[1 + K_2]^{-1} \quad (2)$$

(Consideration of the binding equilibrium for quinone at the Q_B site introduces a quinone concentration dependence into this expression which need not concern us here [20].) In *Rps. viridis,* this relationship has also been utilized, with single component analyses for both $P^+Q_A^-$ and $P^+Q_B^-$ decay [13]. Although the relationship was not as extensively tested as it has been in *Rb. sphaeroides* [12], independent measures of K_2 obtained from cytochrome oxidation on the first and second flashes in *Rps. viridis* agreed well with those determined from the recombination kinetics, at high pH where the cytochrome assay could be used [13]. Thus, any contribution from the direct $P^+Q_B^-$ recombination pathway must be small and there seems to be little reason to doubt that Eqn. 2 is appropriate in this species, also.

We used the fast and slow components of the $P^+Q_A^-$ and $P^+Q_B^-$ recombination kinetics to give two values for K_2, as a function of temperature and pH. In all cases the values of K_2 obtained in a given preparation, utilizing fast or slow components, agreed closely – within a factor of 1.5 – and displayed essentially identical dependences. This strongly suggests that the root cause underlying the heterogeneity of the kinetics does not significantly affect the energetics of the Q_A to Q_B electron transfer equilibrium ($\Delta\Delta G \leqslant 10$ meV) and we may conclude that the biphasicity of the $P^+Q_B^-$ decay arises only as a result of the intrinsic complexity of the $P^+Q_A^-$ decay. We therefore take the rates of recombination of $P^+Q_A^-$ and $P^+Q_B^-$ as good sources of K_2, according to Eqn. 2, and examine this factor as a function of various external parameters.

The temperature dependence of the recombination rates and K_2

The activated nature of the $P^+Q_A^-$ recombination in *Rps. viridis* has been previously interpreted as indicating a route via P^+I^- as an intermediate state, and the temperature dependence was used to determine the energy and free energy gaps between $P^+Q_A^-$ and P^+I^-

TABLE I

Activation parameters for the fast and slow components of the kinetics of recombination of $P^+Q_A^-$ via P^+I^- in isolated RCs of Rps. viridis

Activation parameters determined from the $P^+Q_A^-$ decay kinetic data of Fig. 2, analysed according to Eqn. 3 with $k_d = 2 \cdot 10^7\ s^{-1}$.

Component	$k_{T,i}$ [a] (s^{-1})	$\Delta H^\dagger$ (eV)	$\Delta S^\dagger$ (meV/deg)	$-T\Delta S^\dagger$ [b] (eV)	$\Delta G^\dagger$ (eV)
k_{QA}^{fast}	460	0.280 ±0.004	0.135 ±0.016	−0.040 ±0.005	0.240 ±0.006
k_{QA}^{slow}	155	0.300 ±0.008	0.041 ±0.029	−0.012 ±0.008	0.288 ±0.011

[a] $k_{T,i}$ is the temperature independent rate observed below 200 K. The values of $k_{T,fast}$ and $k_{T,slow}$ are taken from Ref. 9. The error in $k_{T,slow}$ is small (±20 s^{-1}), but $k_{T,fast}$ could lie in the range 400–600 s^{-1}. These uncertainties are not included in the errors quoted in the table.

[b] $T = 296$ K.

[6,9]. Each component was analysed according to a modification of Eqn. 1:

$$k_{QA^i} = k_d \cdot \exp(-\Delta G_i^\dagger / k_b T) + k_{T,i} \quad (3)$$

where the sub(super)script i indicates fast or slow components. Using values for $k_{T,fast} = 460\ s^{-1}$ and $k_{T,slow} = 155\ s^{-1}$ [9], we obtain activation enthalpies of 0.28 eV and 0.30 eV for k_{QA}^{fast} and k_{QA}^{slow}, at pH 8.5, in reasonable agreement with the earlier values of 0.28 and 0.26 eV, respectively, obtained with LDAO as detergent in place of Triton X-100 [9]. Taking $k_d = 2 \cdot 10^7\ s^{-1}$, the entropic contribution was obtained from the extrapolated intercept at $1/T \to 0$, and the resulting activation free energies were $\Delta G_{fast}^\dagger = 0.24$ eV and $\Delta G_{slow}^\dagger = 0.29$ eV, compared with 0.26 and 0.29 eV in our earlier study [9]. The activation parameters are summarized in Table I. There is generally good agreement with our earlier data on isolated RCs in LDAO [9] and with the recent work of Baciou et al. [17] on RCs incorporated into phospholipid vesicles, especially when considering the free energies of activation ($\Delta G_i^\dagger$). The distribution of the free energy between enthalpic and entropic terms, however, is more variable and appears to be sensitive to the environment [17]. The range of properties we have observed for 'fast' and 'slow' RC preparations lies within the range of these 'environmental' influences.

The temperature dependence of K_2 was obtained from the kinetic data, using the relationship of Eqn. 2. At pH 8.5, the two values calculated from the fast and slow components of each back reaction process show a constant difference of less than 50% ($\Delta\Delta G \leqslant 10$ meV). Both estimations yielded very similar slopes equivalent to $\Delta H^\circ(\text{fast}) = -0.360 \pm 0.013$ eV and $\Delta H^\circ(\text{slow}) = -0.352 \pm 0.014$ eV, and intercepts equivalent to $\Delta S^\circ(\text{fast}) = -0.75 \pm 0.22$ meV/deg and $\Delta S^\circ(\text{slow}) = -0.76 \pm 0.25$ meV/deg. At pH 8.5 and ambient temperatures, the full range of values for K_2 in different preparations was 90 to 240, equivalent to $\Delta G^\circ \approx -0.13$ eV. The electron transfer from $Q_A^-Q_B$ to $Q_AQ_B^-$ is accompanied by a large entropy decrease ($\Delta S^\circ \approx -0.8$ meV/deg) and it is likely that events associated with proton binding to the protein contribute a significant portion of this.

The consistency in the values and thermodynamic properties of K_2 determined from the fast and slow components of the $P^+Q_A^-$ and $P^+Q_B^-$ decays, suggests that the heterogeneity arises from differences in the activated recombination route, particularly the energy level of P^+I^-. Thus, the activation free energy from $P^+Q_A^-$ is modulated without altering the free-energy difference between Q_A and Q_B. In contrast to the kinetic heterogeneity within a given preparation, the kinetic differences between the two types of preparation observed in the $P^+Q_A^-$ and cyt $c^+Q_A^-$ recombination kinetics, but not in the $P^+Q_B^-$ decay, suggest that the distinction lies in the effective energy level of the $P^+Q_A^-$ state. After subtraction of the $k_{T,i}$ which do not vary significantly between preparations, the $P^+Q_A^-$ recombination rates observed in 'fast' preparations indicate a free-energy shift of 20–25 mV for $P^+Q_A^-$. Raising the energy level of this state decreases the activation free energy and accelerates the thermal part of the $P^+Q_A^-$ recombination but increases the free energy drop for electron transfer to Q_B, i.e., K_2. The net result (see Eqn. 2) is little or no effect on the rate of $P^+Q_B^-$ decay. Recombination from the cyt $c^+Q_A^-$ state, however, which also proceeds via $P^+Q_A^-$, but by reverse electron transfer equilibrium from P to cyt c^+ [16], will be directly affected by any change in k_{QA}.

pH dependence of the rate of $P^+Q_A^-$ recombination

In our previous studies of the $P^+Q_A^-$ recombination reaction we considered that the pH dependence of the rate arose from differential influences of some protonation sites on I^- and Q_A^-, so that the energy gap between the $P^+Q_A^-$ and P^+I^- states was modulated by pH, thereby varying the contribution of the thermally activated decay route [6,9]. Most protonation reactions are rapid bimolecular processes, but we considered that heterogeneity of the kinetics could arise from this source because the decay of $P^+Q_A^-$, in this species, is fast enough to compete with the protonation equilibrium, and could prevent effective averaging of the kinetics. The fact that we now find the heterogeneity to be still apparent in the decay of $P^+Q_B^-$, on the time scale of 0.1–1 s, shows that the primary source is not a diffusion limited protonation equilibrium, but arises from the existence of 'fast' and 'slow' states of the reaction center that are interconvertible but remain distinct on the time scale of the recombination processes. Within these conformational substates, however, other in-

fluences of protonation equilibria can be experienced directly and rapidly, allowing modulation of the $Q_A^- Q_B \leftrightarrow Q_A Q_B^-$ electron transfer equilibrium (K_2).

The quantitative deviation between the relative amplitude of the fast components in the $P^+Q_A^-$ and $P^+Q_B^-$ kinetics at high pH (Fig. 3) is consistent with our earlier suggestion that the $P^+Q_A^-$ recombination is sufficiently fast to compete with quite rapid protonation equilibria. Thus, at high pH, the apparent amplitude of the fast phase of the $P^+Q_A^-$ decay may be enhanced (relative to $P^+Q_B^-$) because protonation equilibria become generally slower, introducing an additional complexity to the kinetics. With this proviso at high pH, the two distinct components of the k_{QA} data of Fig. 3 may each be described by assigning different k_{QA} values to several relevant protonation states in quasi-equilibrium. For each of the two phases of recombination, the data call for a minimum hypothesis of three independent protonation sites, resulting in eight distinct states (Fig. 5). If all protonation states are considered to be in rapid equilibrium on the timescale of the $P^+Q_A^-$ recombination process, the observed rate is the weighted average of the eight intrinsic recombination rates, k_A through k_H. (The index i, specifying fast or slow component, is omitted for clarity):

$$k_{QA} = \left[\{k_A + k_B(H^+)/K_1\} + \{k_H + k_C(H^+)/K_1\} \cdot (H^+)/K_2 + \{k_E + k_F(H^+)/K_1\} \cdot (H^+)/K_3 + \{k_G + k_D(H^+)/K_1\} \cdot (H^+)^2/K_2K_3 \right] \times \left[\{1+(H^+)/K_1\} \cdot \{1+(H^+)/K_2\} \cdot \{1+(H^+)/K_3\} \right]^{-1} \quad (4)$$

In practice, however, if the pK values are significantly different ($\Delta pK > 0.5$), the equilibrium distribution over the entire pH range is dominated by four states. If none of the minor states has an exceptionally large intrinsic k_{QA} value, i.e., k_E, k_F, k_G, k_H not much larger than k_A, k_B, k_C, k_D, the average rate may be well approximated by:

$$k_{QA} = \frac{k_A + (H^+)/K_1 \cdot [k_B + (H^+)/K_2 \cdot \{k_C + k_D \cdot (H^+)/K_3\}]}{\{1+(H^+)/K_1\} \cdot \{1+(H^+)/K_2\} \cdot \{1+(H^+)/K_3\}} \quad (5A)$$

$$= \frac{k_A + 10^{(pK_1 - pH)} \cdot [k_B + 10^{(pK_2 - pH)} \cdot \{k_C + k_D \cdot 10^{(pK_3 - pH)}\}]}{\{1+10^{(pK_1 - pH)}\} \cdot \{1+10^{(pK_2 - pH)}\} \cdot \{1+10^{(pK_3 - pH)}\}} \quad (5B)$$

This is equivalent to the expression derived earlier [9] *. The curves of Fig. 3 can be generated using Eqn. 5B, by fitting individual values to k_A, k_B, k_C and k_D and to

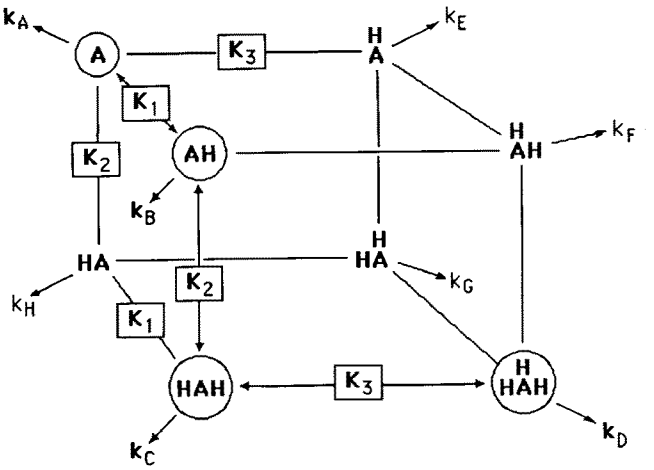

Fig. 5. Generalized scheme accounting for the pH dependence of k_{QA}. Three protonatable groups are considered, generating one fully deprotonated state, three monoprotonated and three diprotonated states, and one fully protonated state. If the three groups are independent, as considered in the text, then $K_i = K_i'$. Each state can be assigned a different intrinsic recombination rate constant (k_A through k_H), giving rise to Eqn. 4 as a complete description of the observed k_{QA} if all states are in rapid equilibrium. However, if the three independent equilibria are distinctly different (pK values different by 0.5 pH units, or more) the equilibria are dominated by 3 of the 12 possible steps (with arrow heads) and 4 of the 8 states (circled), with k_A through k_D. If none of the non-major states has an unusually large intrinsic rate constant, we obtain Eqn. 5.

the protonation equilibria, pK_1, pK_2, pK_3. Alternatively, in terms of Eqn. 3, the different values for k_A through k_D imply modulations (∂G) in $\Delta G^\dagger$, as a result of the differential effects of each ionization state on Q_A^- and I^-. These modulations are obtained after subtracting out the low temperature, activationless rates, $k_{T,fast}$ and $k_{T,slow}$, which are not significantly pH-dependent [9], e.g., for the transition between k_A and k_B:

$$k = k^\ddagger \cdot \frac{\exp(-\partial G_1/k_bT) + 10^{(pH - pK_1)}}{1 + 10^{(pH - pK_1)}} + k_{T,i} \quad (6)$$

Where $k^\ddagger$ is the activated component of the high pH limit value of k (k_{QA}), as given by Eqn. 3: $k^\ddagger = k_d \cdot \exp(-\Delta G^\dagger_{A,i}/k_bT)$. k^{obs} approaches $k_A = k^\ddagger + k_{T,i}$, and $k_B = k^\ddagger \cdot \exp(-\partial G_1/k_bT) + k_{T,i}$ in the high and low pH limits, respectively. The fitting parameters for the $P^+Q_A^-$ data of Fig. 3 are summarized in Table II. The most noteworthy feature is the similarity in pK values describing both the fast and slow phases of the $P^+Q_A^-$ recombination. This, of course, is evident in the general similarities of the two pH dependences, and suggests

* The expression given in Ref. 9 is complementary to Eqn. 5B, in the use of a low pH reference state. A high pH reference – the fully deprotonated state – is heuristically preferable in allowing the conceptual addition of protons sequentially, but it is not always experimentally accessible.

that the slow conformational equilibrium responsible for the basic heterogeneity does not markedly affect the pK values of local groups modulating the $P^+Q_A^-/P^+I^-$ energy gap.

The pH dependence of K_2

The close similarity between the relative amplitudes of the components in the analyses of the $P^+Q_A^-$ and $P^+Q_B^-$ recombination kinetics and the near equivalence of the corresponding K_2 values calculated from the fast and slow phases of each, provide strong support for the origin of the heterogeneity in the $P^+Q_A^-$ recombination and, consequently, the essentially homogeneous nature of the electron transfer from Q_A^- to Q_B. The pH dependence of K_2 reflects the differential interactions of ionizable groups with Q_A/Q_A^- and Q_B/Q_B^-, affecting the electron transfer equilibrium. This is significantly more complex in *Rps. viridis* than has been reported for RCs from *Rb. sphaeroides* [12,21,22]. In contrast to the latter species, where K_2 decreases monotonically as the pH is raised, in *Rps. viridis* it undulates and actually increases over the range pH 8 to 10 (Fig. 6, bottom). Recognizing that the semiquinones themselves are not protonated [23], and using the formalism developed for *Rb. sphaeroides* [12], the pH dependence can be described by various protonation states of the protein that differentially stabilize $Q_A^-Q_B$ or $Q_AQ_B^-$. Thus, it is assumed that the protonation equilibria are established rapidly on the time scale of the recombination kinetics, so that the recovery of P is averaged over the various protonation states. For a single ionizable group, we have:

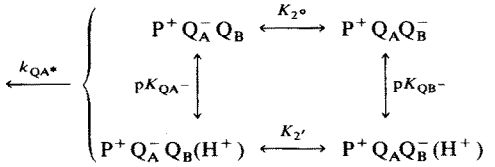

Scheme II.

Where K_2' is the limiting value of the equilibrium constant at low pH. This is merely an extension of the formalism used for describing the $P^+Q_B^-$ recovery kinetics in terms of rapid electron transfer equilibrium between $Q_A^-Q_B$ and $Q_AQ_B^-$ with recombination occurring from $P^+Q_A^-$ (Eqn. 2). The observed recombination rate

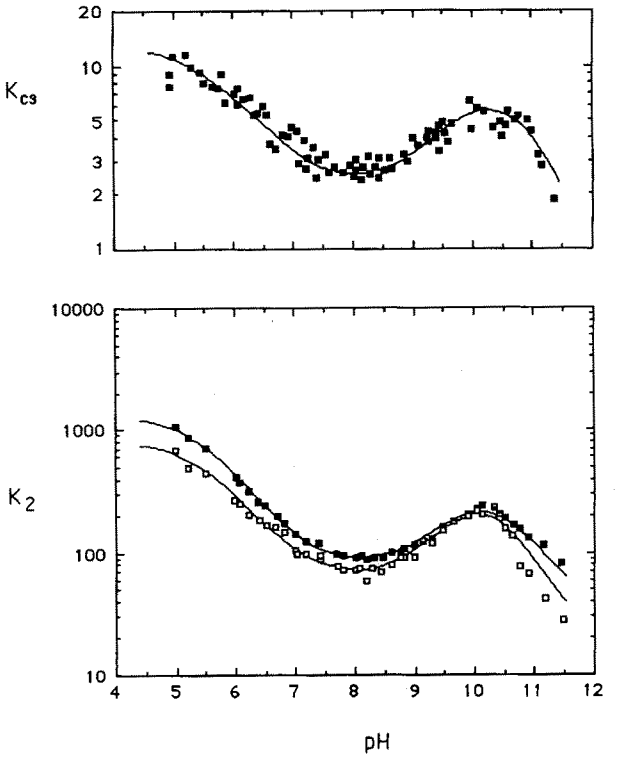

Fig. 6. Bottom panel: pH dependence of the apparent electron transfer equilibrium constant, K_2, between $Q_A^-Q_B$ and $Q_AQ_B^-$, derived from the rate data of Fig. 3 (fast, ■; slow, □). Top panel: pH dependence of the apparent equilibrium constant between fast and slow recombination states of the reaction center, $K_{cs} = C_s/C_f$ (see text); the points are derived from the amplitude data of Fig. 1. The curves are drawn according to Eqn. 9 (K_2) and Eqn. 10 (K_{cs}) for the influence on the equilibrium constants of four independent ionizable groups, as described in the text, with parameters given in Tables III and IV.

TABLE II

pH-dependence parameters for the $P^+Q_A^-$ recombination reaction in isolated RCs from Rps. viridis [a]

Component	$k_{T,i}$ [b] (s^{-1})	k [c,f] (s^{-1})		pK [d,f]	∂G [e,f] (meV)
k_{QA}^{fast}	460	k_A:	3100	9.9 (pK_1)	+17
		k_B:	1800	9.0 (pK_2)	+23
		k_C:	1000	5.6 (pK_3)	−27
		k_D:	2000		
k_{QA}^{slow}	155	k_A:	685	10.05 (pK_1)	+11
		k_B:	500	9.1 (pK_2)	+18
		k_C:	325	5.5 (pK_3)	−22
		k_D:	500		

[a] Parameters derived from analysis of the data in Fig. 3, using Eqns. 5B and 6.

[b] See note b, Table I.

[c] k_A through to k_D are the intrinsic recombination rate constants of the four dominant protonation states described by Eqns. 4 and 5 and illustrated in Fig. 5.

[d] pK_1, pK_2 and pK_3 are defined by Fig. 5 and Eqns. 5B and 6.

[e] ∂G is the difference in free energies of interaction between I^- or Q_A^- and the protonation site characterized by pK_1, pK_2 and pK_3. A positive value implies that protonation stabilizes $P^+Q_A^-$, increases the free energy gap between $P^+Q_A^-$ and P^+I^-. Thus, the recombination rate decelerates and the pH decreases.

[f] The uncertainty in the $k_{T,fast}$ and $k_{T,slow}$ values affects the net rates for each decay channel (k_A through k_D) but does not affect the pK values (pK_1 through pK_3). Since the uncertainty in the k_T values affects all net rates in the same way, the influence on ∂G, which is related to the differences in the rates, is minimal (< 2 mV).

for $P^+Q_B^-$ then follows the pH dependence of the apparent electron transfer equilibrium constant:

$$k_{QB} = k_{QA}[1 + K_2^{app}]^{-1} \quad (7)$$

where *,

$$K_2^{app} = K_2' \cdot \frac{1 + 10^{pH - pK_{QB^-}}}{1 + 10^{pH - pK_{QA^-}}} \quad (8)$$

For several groups (j), all contributing independently to the overall pH idependence, Eqn. 8 is expanded to [21]:

$$K_2^{app} = K_2' \cdot \prod_j \frac{1 + 10^{pH - pK_{QB^-,j}}}{1 + 10^{pH - pK_{QA^-,j}}} \quad (9)$$

As the electron is transferred from Q_A to Q_B, certain ionizable residues experience pK shifts and undergo changes in their degree of ionization. As has been suggested for the light-induced protonation of RCs from *Rb. sphaeroides* [22], proton binding in a particular pH region may reflect the summed response of several groups all undergoing small changes in their net protonation state, rather than a large change in a single residue. However, the two cases are not distinguishable in the present context and it is simpler to speak in terms of 'effective residues' with single pK values and well-defined pK shifts, except where mechanistic distinctions are to be made. The K_2 data can be reasonably well fit with three pK values, but the drawn-out nature of the data at low pH is better fit with an additional component, and the curves drawn in Fig. 6 (lower panel) employ four independent ionizable groups. The pK values used are shown in Table III. The fitting parameters for the three-component fit are also given in the table, for comparison with the fits to the k_{QA} data (Table II).

At low pH, K_2 is large and the electron transfer equilibrium strongly favors $Q_AQ_B^-$ over $Q_A^-Q_B$. As the pH is raised, K_2 decreases, indicating the ionization of an effective residue which, when protonated, stabilizes (interacts with) the electron on Q_B^- more than on Q_A^- ($pK_{QB^-} > pK_{QA^-}$). Below pH 7.0, there appear to be two effective groups with pK_{QA^-} values of about 5.5 and 6.3, and pK_{QB^-} values of about 5.9 and 7, respectively. Between pH 8.5 and 10, another effective residue exerts an opposite effect: the pK for $Q_A^-Q_B$ is about 10.1 and for $Q_AQ_B^-$ is about 9.1. Thus, protonation of this group stabilizes the electron more on Q_A^- than Q_B^-. These relative pK values, i.e., $pK_{QA^-} > pK_{QB^-}$, indicate that there should be proton release in this pH range, as the electron is transferred from Q_A to Q_B. This has yet to be demonstrated. Finally, at high pH a fourth group comes into play which stabilizes the electron on Q_B again, with pK values of approximately 10.2 and ≥ 11.3 for the $Q_A^-Q_B$ and $Q_AQ_B^-$ states, respectively. The noticeable difference between the high pH behavior of the fast and slow component K_2 values may be real, but it is also a region in which the RCs are unstable and the difference is probably within the error of the measurements at high pH. Consistent with this, the limiting slope of the K_2(fast) dependence at high pH is steeper than can be accounted for by a single, group.

TABLE III

pH-dependence parameters for the $Q_A^-Q_B/Q_AQ_B^-$ electron transfer equilibrium [a]

Components [b]	K_2'	pK_{QA^-}	pK_{QB^-}	ΔpK [c]
K_2(fast)	800	10.2	11.9	≥ 1.7
		10.1	9.1	−1.0
		6.3 (5.6) [d]	6.95 (6.7)	0.65 (1.1)
		5.4	5.85	0.45
K_2(slow)	1300	10.2	11.3	1.1
		10.1	9.2	−0.9
		6.2 (5.5)	6.95 (6.7)	0.75 (1.2)
		5.4	5.85	0.45

[a] The parameters of the apparent equilibrium constant are defined by Eqn. 9.

[b] K_2(fast) and K_2(slow) are obtained from the ratio of the respective rate constants (fast or slow) for the components of the $P^+Q_A^-$ and $P^+Q_B^-$ decay kinetics, as given in Eqn. 2.

[c] $\Delta pK = pK_{QB^-} - pK_{QA^-}$.

[d] The values in parentheses show the fitting parameters for the low-pH region using only three components in all – a single effective group replaces the two lowest pK groups of the four component fit. The two higher pK groups are not significantly affected.

Salt dependence of K_2 and k_{QA}

The salt dependences ofo the $P^+Q_A^-$ and $P^+Q_B^-$ recombination reactions are distinct (Fig. 4). The former process accelerates slightly at high ionic strength, while the latter gets slower. This results in a significant salt dependence of the electron transfer equilibrium between $Q_A^-Q_B$ and $Q_AQ_B^-$ (Fig. 7, lower panel). At pH 8.5, K_2 increased from a value of 200 in 10 mM NaCl, to 1200 in 2 M NaCl. High salt effects on the kinetics of proton binding and electron transfer in RCs from *Rb. sphaeroides* have been successfully modelled using a crude Gouy-Chapman approach (Maróti, P. and Wraight, C.A., unpublished observations), implying that the effect is via the mobile counter ion distribution at the surface of the protein and the resulting surface potential and surface pH. It is reasonable to interpret the effect on K_2, seen here, in a similar manner. Thus,

* An equivalent expression may be written in terms of K_2°, i.e., using the fully deprotonated state as the reference point. However, for these data, the end point at high pH is generally less clear than at low pH and it is more straightforward to fit the data by assuming a plateau value at the low pH extremum.

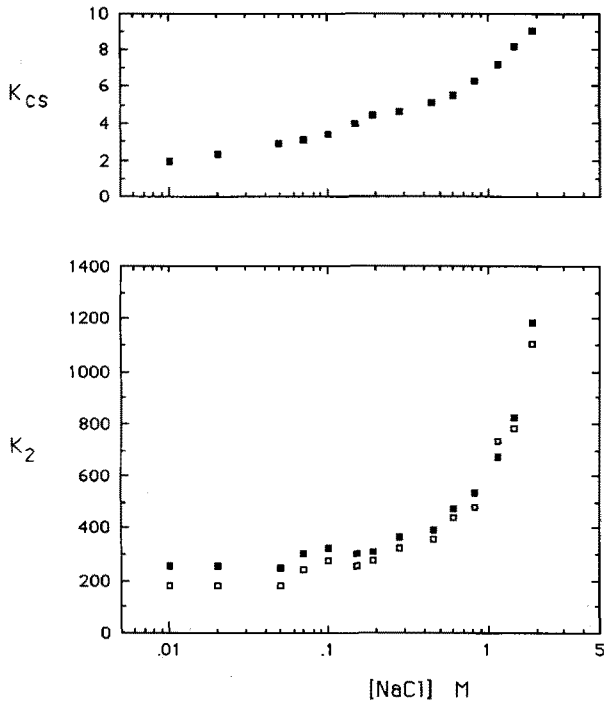

Fig. 7. Bottom panel: Salt dependence of the apparent electron transfer equilibrium constant, K_2, between $Q_A^- Q_B$ and $Q_A Q_B^-$, derived from the data of Fig. 4. Top panel: Salt dependence of the apparent equilibrium constant between fast and slow recombination states of the reaction center, $K_{cs} = C_s/C_f$.

high concentrations of cations at the protein surface stabilize Q_B^- more than Q_A^-, implying that the Q_B site is more accessible or otherwise more under the influence of the surface charge and the solvent dielectric. From the X-ray structure it is clear that the Q_B site is more polar and contains a number of water molecules [24]. It is also connected to the aqueous environment in order to allow proton uptake in the formation of fully reduced quinol. The nature of this connection is uncertain at the present time, but a proton-conducting, hydrogen-bonded network is a widely considered possibility [24,25].

The salt dependence of the $P^+Q_A^-$ recombination rate constants also indicates a differential solvent or screening effect on the stability of I^- and Q_A^-, and may be, at least partly, effected via the surface pH and the ionization state of surface groups. Since the rates of both components increase with increasing salt concentration, the energy gap between $P^+Q_A^-$ and P^+I^- would appear to be decreasing, implying that the latter is relatively more stabilized in high salt. This may imply that I is more exposed that Q_A, possibly as an artifact of the isolated nature of the RC. However, the narrowing of the energy gap could reflect *de*stabilization of Q_A^- due to screening of the surface potential. This would raise the surface pH, leading to further ionization of surface groups and an increase in the (negative) surface charge.

The origin of the heterogeneity of charge recombination: pH dependence of the amplitudes

The essential similarity of the two sets of K_2 values calculated from the fast and slow components, respectively, of the $P^+Q_A^-$ and $P^+Q_B^-$ decay kinetics suggests that these states of the RC refer to the intrinsic behavior of the $P^+Q_A^-$ recombination with little distinction at the level of the $Q_A^- Q_B / Q_A Q_B^-$ equilibrium. We suggest, expanding our earlier proposal [9], that the biphasic kinetics of decay of both $P^+Q_A^-$ and $P^+Q_B^-$ in *Rps. viridis* RCs arise from a slow equilibrium between two states of the RC differing in the energy level of the intermediate state, P^+I^- *. In principle, the essential phenomenon reported here – very similar biphasicities of the $P^+Q_A^-$ and $P^+Q_B^-$ decay kinetics over a wide range of conditions – could be explained by independent but cancelling, effects on the energetics of the $P^+Q_A^-$ and $P^+Q_B^-$ states. The recombination kinetics would then reflect the energy level of $P^+Q_A^-$ only (reacting via P^+I^-), as the value of K_2 would remain fortuitously constant. However, this is extremely unlikely as a major source of the effect because, in the case of the pH dependences, many ionizable groups must be responsible over the whole pH range, and these can hardly all be expected to have identical influences on $P^+Q_A^-$ and $P^+Q_B^-$. In contrast, an influence on P^+I^-, as a common intermediate to both decay processes, is relatively easy to accept. (The small differences between the two sets of K_2 values, amounting to less than 15 mV, may reflect subtle distinctions in the interactions with Q_A and Q_B.)

For simplicity, we consider the kinetic components as arising from two conformational states or conformers, 'fast' and 'slow', in slow equilibrium with each other before the flash:

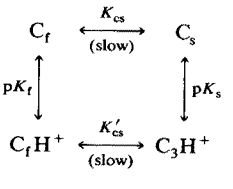

Scheme III.

where subscripts f and s refer to the fast and slow recombining conformers. The fact that the fraction of either component does not titrate to 1 in a simple pH dependence requires a minimal scheme for the protona-

* We have recently found an earlier report of biphasic kinetics for $P^+Q_A^-$ decay in *Rb. sphaeroides*, described by Lukshene et al. [34] in terms of a slow equilibrium between two conformational states of differing intrinsic kinetics. In *Rb. sphaeroides*, however, the decay is via a direct tunneling from Q_A^- to P^+, and does not proceed via an activated route at any temperature. The slow component became dominant at low temperatures, as in *Rps. viridis*, but the relationship between the temperature-dependent and temperature-independent phenomena is currently obscure.

TABLE IV

pH-dependence parameters for the conformational equilibrium

The parameters are defined by Scheme III and Eqn. 10.

K'_{cs}	$pK_{f,j}$	$pK_{s,j}$	ΔpK [a]
13	10.6	11.8	>1.2
	9.85	9.25	−0.6
	6.5 (5.8) [b]	6.9 (6.45)	0.4 (0.65)
	5.4	5.7	0.3

[a] $\Delta pK = pK_s - pK_f$.

[b] The values in parentheses show the fitting parameters for the low-pH region using a total of only three components – a single effective group replaces the two lowest-pK groups of the four component fit. The two higher-pK groups are not significantly affected.

tion dependent equilibria, as above, with the two conformational equilibrium constants, K_{cs} and K'_{cs}, not greatly different from 1 and the difference in pK values small. The data require the consideration of several groups. If these act independently to influence the conformational equilibrium, the apparent equilibrium constant is described by the same type of expression as given above for K_2 (Eqn. 9):

$$K_{cs}^{app} = K'_{cs} \cdot \prod_j \frac{1+10^{pH-pK_{s,j}}}{1+10^{pH-pK_{f,j}}} \qquad (10)$$

The amplitude data of Fig. 3 are shown as K_{cs} in Fig. 6 (top panel). The curves are drawn according to Eqn. 10, utilizing four independent groups with pK values as given in Table IV. A somewhat less satisfactory fit could also be made with only three groups; this is also given in the table, for comparison with the three component fits to the k_{QA} and K_2 data.

This description of the heterogeneity should yield identical behavior for the relative amplitudes of the phases in the $P^+Q_A^-$ and $P^+Q_B^-$ recombination kinetics. This is not fully supported by the data of Fig. 3 (top), which shows the fast phase of the $P^+Q_A^-$ recombination to be significantly larger than that of the $P^+Q_B^-$ recombination above pH 8. Rather than abandon the simplicity of the current scheme, we recall the earlier suggestion of Sebban and Wraight [9] to account for the additional biphasicity seen in the $P^+Q_A^-$ decay at high pH. At high pH the fast kinetics of the $P^+Q_A^-$ decay occur on the same time-scale as the re-equilibration of protonation states after the flash. As the protonation equilibria get progressively slower at high pH, the kinetics of $P^+Q_A^-$ recombination become inherently polyphasic and the bi-exponential analysis yields larger fast phase amplitudes.

The conformational equilibrium responsible for the heterogeneity must be slow on the time scale of the $P^+Q_B^-$ recombination ($t_{1/2} \leqslant 0.5$ s) and we have attempted to determine the relevant time scale by following the kinetics at various times after a pH jump from 6 to 8.5. Within the limits of the mixing and settling time, we can only say that the transition is 95% complete at about 10 s. This places the time constant for the conformational change in the same range as the $P^+Q_B^-$ recombination. Thus, some of the discrepancy between the amplitudes of the $P^+Q_A^-$ and $P^+Q_B^-$ recombination phases may arise from the $P^+Q_B^-$ kinetic analysis.

The protonation equilibria, to which the conformational change is linked, need not be slow and some of the same groups could be involved in the rapid equilibration responsible for the pH dependence of K_2 or of k_{QA}. This may underlie the close resemblance of the pH dependence of the amplitudes of the fast components and the pH dependence of the electron transfer equilibrium constant (Figs. 3 and 6). Although there are definite regions of the pH scale where many different residues can be expected to have their pK values, the similarity in shape of the two curves, for K_{cs} and K_2, could be more than just coincidence and we should consider the possibility that some of the residues that affect the $P^+Q_A^-$ recombination kinetics *do* influence the $Q_A^-Q_B/Q_AQ_B^-$ equilibrium. For example, some residues that influence the energetics of the $Q_A^-Q_B/Q_AQ_B^-$ equilibrium by their rapid protonation, may also be linked to slow conformational changes that modulate the activity of P^+I^- in the $P^+Q_A^-$ recombination. The scheme of Fig. 8 shows the essential features of this hypothesis, for a single protonatable residue. The conformational equilibrium is established slowly prior to light activation according to the pK values and equilibria of the dark-adapted state – pK_f, pK_s, K_{cs} and K'_{cs}. Following a flash, electron transfer and charge

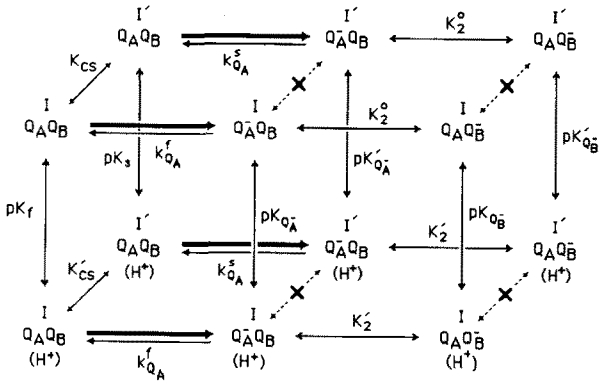

Fig. 8. Scheme showing the generation of fast and slow recombining states of the reaction center via a slow, protonation-linked conformational change. A single ionizable group is considered here. The front panel represents fast states, the back panel shows slow (I-prime) states. Conformational equilibrium is established in the dark, but is too slow to allow reequilibration during the lifetime of the charge separated states, as indicated by the X's The scheme shows how an ionizable group that regulates the slow conformational equilibrium between I and I′ states could also be involved in the rapid equilibrations of the electron transfer between Q_A and Q_B.

recombination occur much faster than the conformational equilibria and the 'fast' and 'slow' channels proceed essentially independently.

The temperature dependence of the heterogeneity

The involvement of P^+I^- in the activated recombination path is dependent on the energy gp between P^+I^- and $P^+Q_A^-$, which is determined by the effective redox potentials of I/I^- and Q_A/Q_A^-. A simple explanation for the two kinetic phases might be that they arise from conformational states with slightly different energy gaps between P^+I^- and $P^+Q_A^-$, with the fast phase manifesting a smaller gap. The difference between the activation parameters of the two phases, as revealed by analysis with Eqn. 3, is consistent with this (Table I: $\Delta\Delta H^\dagger = 20$ meV, $\Delta\Delta G^\dagger = 50$ meV). The amplitude of the slow phase of $P^+Q_B^-$ recombination increased as the temperature was lowered, following the same trend as for the $P^+Q_A^-$ reaction, which is at least 90% slow below about 250 K [9]. When expressed as an equilibrium between two conformers: $C_f \leftrightarrow C_s$, the apparent equilibrium constant (K_{cs}), at pH 8.5, is about 1.5 at room temperature ($\Delta G° = -10$ meV) and displays a weak temperature dependence equivalent to $\Delta H° = -60$ meV and $\Delta S° = -0.17$ meV/deg (Fig. 2, top). The enthalpy of this equilibrium represents the energy splitting between the two conformers in the dark-adapted state. These parameters indicate that the conformer responsible for the slow phase is of lower enthalpy and free energy than the fast conformer. This is not in simple support of an energetic origin of the two components, although the energy splitting of the conformers in the ground state need not be the same as that for the charge separation states.

The fact that the difference in the activation parameters of the two phases and the temperature dependence for the amplitude ratio are all small raises the possibility that a substantial contribution to the distinction between the two conformers may not be energetic at all (as analysed above and in Ref. 9) but resides in different values of k_d, the decay rate constant for recombination of P^+I^-. Thus, instead of describing the two phases of the $P^+Q_A^-$ recombination with a single value for k_d as in Eqn. 3, one would use:

$$k_{QA}^i = k_{d,i} \cdot \exp(-\Delta G^\dagger / k_b T) + k_{T,i} \qquad (11)$$

Even more generally, one should incorporate both $k_{d,i}$ and $\Delta G_i^\dagger$. This invites a careful reexamination of the $P^+Q_A^-$ and P^+I^- recombination kinetics, but it is noteworthy that the kinetics of P^+I^- recombination in *Rb. sphaeroides* were considered to be cleanly mono-exponential [26].

If the direct, activationless recombination path is monophasic, the $P^+Q_A^-$ decay kinetics should tend towards monophasic at low temperature, regardless of any equilibrium between fast and slow conformers, as the contribution from the thermally activated route via P^+I^- diminishes. The direct route for the $P^+Q_A^-$ recombination becomes dominant below about 250 K. In view of the inevitable freezing out of the activated process, the residual amount of fast phase seen even at 100 K (10–15% [9]) may have an entirely separate origin.

In *Rb. sphaeorides*, the decay of $P^+Q_A^-$ in native RCs occurs only through the direct activationless path and is generally considered to be monophasic at ambient temperatures *. When the native Q_A (ubiquinone) is extracted and replaced by a low-potential analogue, such as anthraquinone, the back-reaction becomes much faster due to contribution from the thermally activated route. Under such conditions, the kinetics have been reported to become distinctly biphasic [27]. This was originally taken to be consistent with our earlier suggestion that the biphasicity arose, largely, from failure to fully equilibrate the protonation states during the lifetime of the more rapid recombination. In the present context, however, we view it as reflecting the involvement of P^+I^- in the activated recombination route, made accessible by the low potential of the anthraquinone, with heterogenous kinetics arising from distinct conformers of that state. Somewhat perversely, native RCs from *Rb. sphaeroides*, with ubiquinone as Q_A, *do* display biphasic kinetics at low temperature [10]. This is not accounted for by the interpretations of the present work but the possibility that the low-temperature heterogeneity has a distinct origin, as suggested above, can accommodate it, of course. It has been recently proposed that the direct, activationless recombination of $P^+Q_A^-$ in *Rb. sphaeroides* occurs via superexchange with the state P^+I^- [28]. Such a mechanism would provide a means for conformational heterogeneity around the bacteriopheophytin to influence the low temperature recombination as well as the activated process seen in *Rps. viridis* at higher temperatures.

The salt dependence of the heterogeneity

In addition to pH, salt concentration also significantly affected the relative amplitudes of the fast and slow kinetic components of the $P^+Q_B^-$ recombination. This is not surprising as the pK values of most ionizable groups, including those linked to the conformational source of the heterogeneity, are expected to be sensitive to ionic strength and surface potential. At pH 8.5, the apparent equilibrium constant between fast and slow conformers increased from about 2, at low salt concentrations, to 10 at 2 M NaCl. If the effect of salt is exerted entirely through the influence of surface poten-

* See footnote to p. 268.

tial on the apparent pK values of exposed groups, comparison with the pH dependence of K_{cs} in 100 mM NaCl (Fig. 7, top) indicates a shift in surface pH of 1.5–2 pH units in the presence of 2 M NaCl. The substantial magnitude of this change and the high salt concentrations needed imply a large surface potential and surface charge density at zero ionic strength but this is consistent with estimations from the amino acid composition and structure of the RC and with experimental findings for RCs from *Rb. sphaeroides* (Maróti, P. and Wraight, C.A., unpublished observations).

Relationship to other kinetic heterogeneities

The conclusion that the origin of the biphasicity lies in proton-linked conformational states of the RC, via P^+I^-, is especially significant in view of other reports on the behavior of this state at short times. Woodbury and Parson [26] reported that the decay of fluorescence in the nanosecond time range, in RCs with Q_A extracted, was polyphasic. They proposed that P^+I^-, formed as the primary charge separation state, underwent relaxations of several tens of millivolts, so that the probability of reexcitation to the emissive, singlet state decayed progressively, in a complex fashion. A possible source for these relaxations is protein conformational changes. Subsequent studies by Woodbury et al. [8] showed that thermal repopulation of P^+I^- from $P^+Q_A^-$ generated a state that was substantially lower energy than any of the P^+I^- states, initial or relaxed, detected in the forward electron transfer path. A very similar relationship was demonstrated in RCs of *Rps. viridis,* by our previous work [6,9]. This suggests further relaxations of the protein structure during the lifetime of $P^+Q_A^-$, possibly involving proton binding by the protein.

Recently, the possibility of kinetic heterogeneity at very short times has been suggested by a careful analysis of the kinetics of formation and decay of P^+I^-. Kirmaier and Holten [29] report these events to occur with a range of time constants at different measuring wavelengths, formation and decay occurring in 1–4 ps and 100–300 ps, respectively. Their interpretation is that the RC population represents a distribution of conformers that do not rapidly interconvert in the subnanosecond time range. It is well known that as the temperature is lowered both these processes speed up from their average values of about 3 and 200 ps, to about 1 and 100 ps at 4 K (see Ref. 30 for review). Kirmaier and Holten reinterpret this phenomenon as reflecting a narrowing of the distribution into one dominated by the faster reacting conformers. This may arise from a physical contraction of the protein, as suggested earlier [31]. However, this area is open to reevaluation in the light of recent measurements that have apparently resolved the reduction of the monomeric bacteriochlorophyll *en route* to the bacteriopheophytin [32].

Failure to equilibrate conformational substates on the subnanosecond timescale is hardly surprising. However, the persistence of distinct components on the seconds timescale at room temperature implies similarly long-lived conformational states which, although less widely recognized, are nonetheless common, as is evident in the very slow rates of D^+–H^+ exchange in buried amide linkages. In the terminology of Freuenfelder and co-workers [33], these would constitute members of a high level conformational substate tier (CS^0), with large energy barriers between them. Possibilities include a slow secondary structure change following protonation of a more exposed residue.

Although there is no a priori reason why the heterogeneity evident at short and long times should have the same origin, it is possible and certainly tidier given the central role of P^+I^- proposed for both. The fact that the fast reactions become more uniform and faster at low temperature, whereas the $P^+Q_A^-$ recombination reaction becomes monophasically slow is not contradictory to this, as the recombination at low temperature does not involve P^+I^- directly. It would be of interest to determine the primary kinetic rates as a function of pH, but the heterogeneity in the short time domain is likely to arise from a much broader distribution of conformational substates. In the long time domain of the $P^+Q_A^-$ and $P^+Q_B^-$ recombinations, most substates will interconvert rapidly and the distribution is expected to collapse into only a few (e.g., two) high level substates.

Conclusions

Heterogeneity is observed in the kinetics of recombination of the $P^+Q_A^-$ and $P^+Q_B^-$ states, at least out to hundreds of milliseconds. The primary source of this heterogeneity is suggested to be the existence of two (or more) conformational substates of the reaction center that differ in the energy level and/or intrinsic decay properties of P^+I^-, the thermally accessed intermediate in the decay of $P^+Q_A^-$. These conformers, which differ slightly in their spectral properties [9,10], interconvert more slowly than the lifetime of either of the charge separated states and thus the heterogeneity that is intrinsic to the $P^+Q_A^-$ decay is also manifested in the $P^+Q_B^-$ kinetics. The conformational equilibrium is a function of environmental parameters including pH, temperature and salt concentration. The conformational substates do not differ greatly in the energetics of electron transfer between Q_A and Q_B. However, the $Q_A^-Q_B/Q_AQ_B^-$ electron transfer equilibrium does vary with environmental parameters and the pH dependence indicates the involvement of at least four distinct ionizable groups, or ensembles of groups, in interactions

with Q_A^- and Q_B^- that differentially stabilize one over the other. The salt dependences of the electron transfer equilibrium and of the recombination rates, suggest differential effects of the solvent and ionic screening on the stability of I^-, Q_A^- and Q_B^-. A second, and distinct, type of variability in the kinetics of charge recombination is seen between different preparations of RCs, which manifest different rates of $P^+Q_A^-$ and cyt $c^+Q_A^-$ recombination, but similar rates of $P^+Q_B^-$ recombination. This is suggested to arise from modulations of the $P^+Q_A^-$ energy level, alone, possibly by environmental factors (lipid vs. detergent, etc.), which affect the energy gaps between $P^+Q_A^-$ and P^+I^- and between $P^+Q_A^-$ and $P^+Q_B^-$ in a complementary way.

Acknowledgements

This work was supported by grants to C.A.W. from the National Science Foundation (DMB 86-17144 and MDB 89-04991).

References

1 Deisenhofer, J., Epp, O., Miki, K., Huber, R. and Michel, H. (1985) Nature 318, 618–624.
2 Michel, H., Epp, O. and Deisenhofer, J. (1986) EMBO J. 5, 2445–2451.
3 Allen, J.P., Feher, G., Yeates, T.O., Komiya, H. and Rees, D.C. (1987) Proc. Natl. Acad. Sci. USA 84, 5730–5734.
4 Allen, J.P., Feher, G., Yeates, T.O., Komiya, H. and Rees, D.C. (1987) Proc. Natl. Acad. Sci. USA 84, 6162–6166.
5 Shopes, R.J. and Wraight, C.A. (1985) Biochim. Biophys. Acta 806, 348–356.
6 Shopes, R.J. and Wraight, C.A. (1987) Biochim. Biophys. Acta 893, 409–423.
7 Gunner, M.R., Robertson, D.E. and Dutton, P.L. (1986) J. Phys. Chem. 90, 3183–3195.
8 Woodbury, N.W., Parson, W.W., Gunner, M.R., Prince, R.C. and Dutton, P.L. (1986) Biochim. Biophys. Acta 851, 6–22.
9 Sebban, P. and Wraight, C.A. (1989) Biochim. Biophys. Acta 974, 54–65.
10 Parot, P., Thiery, J. and Vermeglio, A. (1987) Biochim. Biophys. Acta 893, 534–543.
11 Wraight, C.A. and Stein, R.R. (1980) FEBS Lett. 113, 73–77.
12 Kleinfeld, D., Okamura, M.Y. and Feher, G. (1984) Biochim. Biophys. Acta 766, 126–140.
13 Wraight, C.A., Shopes, R.J. and McComb, J.C. (1987) in Progress in Photosynthesis Research (Biggins, J., ed.), Vol. II, pp. 387–396, Martinus Nijhoff, Dordrecht.
14 Shopes, R.J. and Wraight, C.A. (1986) Biochim. Biophys. Acta 848, 364–371.
15 Stein, R.R. (1986) Ph.D. Thesis, University of Illinois at Urbana-Champaign.
16 Gao, J.-L., Shopes, R.J. and Wraight, C.A. (1990) Biochim. Biophys. Acta 1015, 96–108.
17 Baciou, L., Rivas, E. and Sebban, P. (1990) Biochemistry 29, 2966–2976.
18 Crofts, A.R. and Wraight, C.A. (1983) Biochim. Biophys. Acta 726, 149–185.
19 Mancino, L.J., Dean, D.P. and Blankenship, R.E. (1984) Biochim. Biophys. Acta 764, 46–54.
20 Wraight, C.A. and Stein, R.R. (1983) in Oxygen Evolving System of Photosynthesis (Inoue, Y. et al., eds.), pp. 383–392, Academic Press, New York.
21 Maróti, P. and Wraight, C.A. (1988) Biochim. Biophys. Acta 934, 329–347.
22 McPherson, P., Okamura, M.Y. and Feher, G. (1988) Biochim. Biophys. Acta 934, 348–368.
23 Wraight, C.A. (1979) Biochim. Biophys. Acta 548, 309–327.
24 Deisenhofer, J. and Michel, H. (1989) EMBO J. 8, 2149–2169.
25 Allen, J.P., Feher, G., Yeates, T.O., Komiya, H. and Rees, D.C. (1988) Proc. Natl. Acad. Sci. USA 85, 8487–8491.
26 Woodbury, N.W. and Parson, W.W. (1983) Biochim. Biophys. Acta 767, 345–361.
27 Sebban, P. (1988) Biochim. Biophys. Acta 936, 124–132.
28 Franzen, S., Goldstein, R.F. and Boxer, S.G. (1991) J. Phys. Chem., in press.
29 Kirmaier, C. and Holten, D. (1991) Proc. Natl. Acad. Sci. USA, in press.
30 Kirmaier, C. and Holten, D. (1987) Photosynth. Res. 13, 225–260.
31 Feher, G., Okamura, M.Y. and Kleinfeld, D. (1987) in Protein Structure: Molecular and Electronic Reactivity (Austin, R. et al., eds.), pp. 399–421, Springer, New York.
32 Zinth, W., Holzapfl, W., Finkele, U., Kaiser, W., Oesterhelt, D., Scheer, H. and Stilz, H. (1989) in Current Research in Photosynthesis (Baltscheffsky, M., ed.), Vol. I, pp. 27–3, Kluwer, Dordrecht.
33 Frauenfelder, H., Parak, F. and Young, R.D. (1988) Annu. Rev. Biophys. Biophys. Chem. 17, 451–479.
34 Lukshene, Z.B., Lukashev, E.P., Lukshas, A.K., Nosov, V.N., Zakharova, N.I., Kononenko, A.A. and Rubin, A.B. (1986) Mol. Biol. (USSR) 20, 233–240.